JOURNAL OF AIRCRAFT
Vol. 43, No. 6, November–December 2006

Multidisciplinary Optimization Framework for Control-Configuration Integration in Aircraft Conceptual Design

Ruben E. Perez* and Hugh H. T. Liu†
University of Toronto, Toronto, Ontario M3H 5T6, Canada
and
Kamran Behdinan‡
Ryerson University, Toronto, Ontario M5B 2K3, Canada

DOI: 10.2514/1.22263

The emerging flight-by-wire and flight-by-light technologies increase the possibility of enabling and improving aircraft design with excellent handling qualities and performance across the flight envelope. As a result, it is desired to take into account the dynamic characteristics and automatic control capabilities at the early conceptual stage. In this paper, an integrated control-configured aircraft design sizing framework is presented. It makes use of multidisciplinary design optimization to overcome the challenges which the flight dynamics and control integration present when included with the traditional disciplines in an aircraft sizing process. A commercial aircraft design example demonstrates the capability of the proposed methodology. The approach brings higher freedom in design, leading to aircraft that exploit the benefits of control configuration. It also helps to reduce time and cost in the engineering development cycle.

Nomenclature

A	=	state matrix
B	=	input matrix
C	=	output matrix
c	=	chord length, ft
$\bar{c}$	=	mean aerodynamic chord, ft
f	=	objective function
I_{yy}	=	pitching moment of inertia, slug-ft^2
J	=	compatibility constraint
K	=	feedback control gain
M	=	pitch moment
n_z	=	normal acceleration, g/rad
p	=	roll rate, deg/s
q	=	pitch rate, rad/s
r	=	yaw rate, deg/s
$\bar{r}$	=	reference signal
S	=	area, ft^2
T	=	engine thrust, lb
tc	=	thickness to chord ratio
t_{pk}	=	response peak time, s
$\bar{u}$	=	control vector
V	=	aircraft velocity, ft/s
x	=	local design variable
$\bar{x}$	=	state vector
y	=	coupling design variable
$\bar{y}$	=	output vector
Z	=	normal force
z	=	global design variable

Subscripts

a	=	aileron
ce	=	control effector
cs	=	control surface
dr	=	Dutch roll
e	=	elevator
eng	=	engine
ht	=	horizontal tail
i	=	ith discipline
ic	=	inner chord
oc	=	outer chord
r	=	rudder
ref	=	reference value
SL	=	system level
sp	=	short period mode
vt	=	vertical tail
w	=	wing
wo	=	washout filter

Symbols

α	=	angle of attack, rad
β	=	sideslip angle, deg
δ	=	deflection, deg
ε	=	constraint tolerance value
ζ	=	damping ratio
η	=	normalized control effector span location
Λ	=	sweep angle, deg
λ	=	taper ratio
τ	=	time constant
ϕ	=	bank angle, deg
ω	=	frequency, rad/s

Received 4 January 2006; revision received 30 June 2006; accepted for publication 15 September 2006.

*Ph.D. Candidate, Institute for Aerospace Studies. Student Member AIAA.
†Associate Professor, Institute for Aerospace Studies. Member AIAA.
‡Associate Professor and Chair, Department of Aerospace Engineering. Member AIAA.

I. Introduction

FLIGHT dynamics and control (FDC) has a significant impact on the aircraft performance and cost [1]. It is also an important discipline for flight safety and aircraft certification. Considerations of dynamic characteristics and control design are essential in the design of future aircraft. Furthermore, the use of control-augmented or control-configured vehicles could offer significant opportunities for

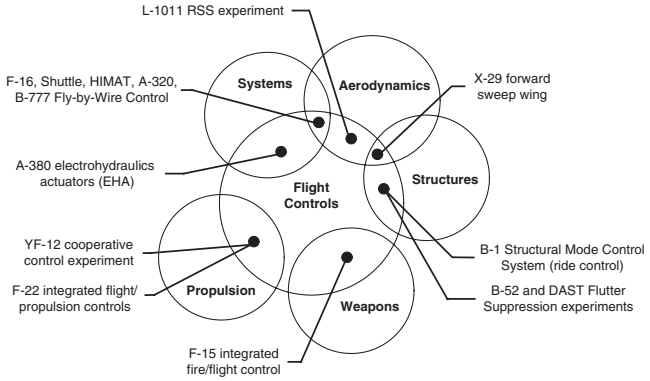

Fig. 1 Examples of flight control integration with traditional disciplines.

expanded flight envelopes and enhanced performance, as demonstrated over the years with different research efforts as shown in Fig. 1 adapted from [2].

In the traditional conceptual design process, the disciplinary analyses are performed sequentially. It is an iterative process in which interdisciplinary trades are used to size the aircraft. With the advances of new technologies such as flight-by-wire and flight-by-light technologies, more emphasis is placed on the analysis of flight dynamics early at the conceptual stage [3,4]. It is of the authors' main interest to study the impact of the aircraft and control surface sizing on flight control capability and dynamic performance. From flight dynamics and control perspective, the classical control surface sizing at the conceptual design stage is primarily limited to the use of the so-called *volume coefficient* [5] which estimates the control surface size based on historical data by assuming the effectiveness of the tail in generating a moment about the center of gravity is proportional to the force (i.e., lift) produced by the tail and its moment arm [6]. Once these control surfaces are sized, limited trim, control, and stability characteristics can be found using single-degree-of-freedom equations [5,7]. In most advanced methods such equations are analyzed over some specific set of flight conditions [8,9]. More explicit considerations of flight dynamics and control are not taken into account until later in the preliminary design stages where much more detailed information about the aircraft has been established.

The challenge is, however, that the sequential process may lead to suboptimal designs due to its inability to capture the interactions between the sizing of control surfaces, their control system, and their effect on the general dynamic behavior of the aircraft. It does not take into account (or take advantage of) the coupling effects between the sizing and the dynamic characteristics. Also, it imposes constraints on control surfaces and limitations on dynamic and control performance, which may be reflected in costly design modifications at later stages in the design chain [10].

To address this challenge, a novel method for the concurrent design of the control system and the aircraft, including the control surface sizing, is presented in this paper. Using a multidisciplinary design optimization (MDO) approach, the control surface sizing with feedback flight control system development is integrated in the conceptual aircraft sizing process. Because more disciplinary aspects of the aircraft are considered simultaneously, better control-augmented aircraft designs can be obtained, based on specified mission parameters, including flight dynamics, handling quality, and control related objectives over the entire aircraft mission profile.

II. Integration Methodology Challenges

Although the benefits of simultaneous considerations of flight dynamics and control in aircraft design have been considered since the 1970s [11], very few efforts have been made over the years to integrate FDC in the conceptual design phases. A number of challenges are given below.

First of all, the aircraft design has to guarantee satisfactory flight characteristics over the entire flight envelope. To ensure positive characteristics, proper control is required for each point within the envelope. The number of analyses required to cover the entire envelope becomes unaffordable at the conceptual stage.

Second, unlike many other disciplines involved in the conceptual design process, FDC does not have an obvious figure of merit (FOM) that can be used for design optimization. For example, drag count is a continuous FOM used in aerodynamics where the disciplinary goal is to minimize such measurement. The challenge lies in the proper specification definition that considers the dynamics and control requirements and constraints simultaneously.

Third, in the current design process very few interactions between the control and the aircraft design processes are taken into account. As a result, when the design has been frozen and information regarding the design matures, so that better disciplinary information is known, any deficiencies in FDC which could be avoided by considering such interactions suddenly become very expensive to fix: they require changes to control surfaces, additional wind tunnel testing to place vortex generators, installation of redundant control systems, etc. The challenge lies in how to enable control-configuration interactions at the conceptual design stage not only to exploit the coupling benefits that arise from such integration but also to reduce any possible FDC deficiencies as early as possible.

A final obstacle is how to deal with the increased data and computational complexity.

III. Flight Dynamics and Control Integration Methodology

The proposed methodology makes use of multidisciplinary optimization to solve the design complexity paradigm while simultaneously designing the aircraft and the control system at different constraining conditions. Details of the proposed solution to flight dynamic and control integration challenges are presented in the following sections.

A. Multidisciplinary Design Integration

With recent advances in the field of MDO [12], it is possible to transform the traditional vertical design process into a horizontal process, enabling concurrent analysis and design. Therefore, it is possible to address the FDC integration/interaction challenge and take advantage of the concurrent structure to increase freedom in the design space. Among many different MDO strategies, collaborative optimization (CO) [13] shown in Fig. 2 has been found to be one suitable alternative to include flight dynamics and control in the design process. CO is a bilevel optimization scheme that decouples the design process by providing the common design variables and disciplinary coupling interactions all at once in an upper level, eliminating the need for an a priori process that accumulates all the disciplinary data required to perform FDC analyses.

At the system level (SL), the collaborative optimization objective function is stated as

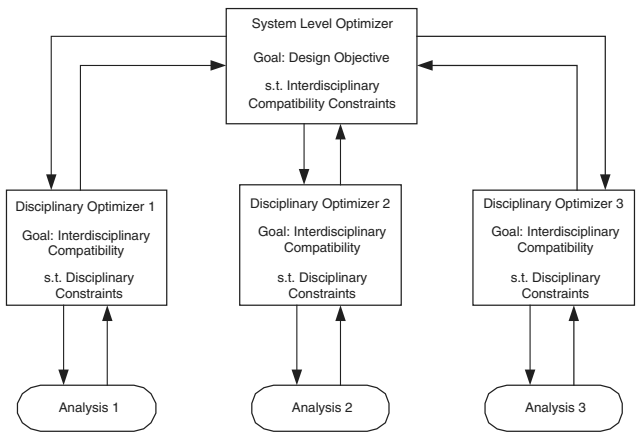

Fig. 2 Collaborative optimization method.

$$\min_{z_{SL},y_{SL}} \quad f(z_{SL}, y_{SL}) \quad \text{subject to}$$
$$J_i^*[z_{SL}, z_i^*, y_{SL}, y_i^*(x_i^*, y_j^*, z_i^*)] \le \varepsilon \qquad i, j = 1, \ldots, n \qquad j \ne i \tag{1}$$

where f represents the system level objective function. J_i^* represents the compatibility constraint for the ith subsystem (of the total n subsystems) optimization problem. Variables shared by all subsystems are defined as global variables (z). Variables calculated by a subsystem and required by another are defined as coupling variables (y). Variables with a superscript asterisk indicate optimal values for the subsystem level optimization. Note that the system level constraint assures simultaneous coordination of the coupled disciplinary values. When using local optimization schemes the MDO mathematical foundation leads to a unique "multidisciplinary feasible point," which is the optimal solution for all disciplines.

The lower-level objective function is formulated such that it minimizes the interdisciplinary discrepancy while meeting local disciplinary constraints. At the disciplinary level, the ith subsystem optimization is stated as

$$\min_{z_i, y_i, y_j, x_i}$$
$$J_i = \sum (z_{SLi} - z_i)^2 + \sum (y_{SL_j} - y_j)^2 + \sum (y_{SLi} - y_i)^2 \tag{2}$$
$$\text{subject to} \qquad g_i[x_i, z_i, y_i(x_i, y_j, z_i)] \le 0$$

where x_i are local subsystem design variables, y_i are subsystem coupling output variables, y_j are subsystem coupling input variables, z_i are the system level variables required by the subsystem discipline analysis, and g_i is the specific disciplinary constraint.

FDC concurrent evaluation becomes available thanks to the nature of the adopted MDO approach. The flight dynamics and control analysis requires parameters from other disciplines, such as lift, drag, stability derivatives, and inertias. Under the bilevel design structure, these parameters are defined as coupling variables and are provided simultaneously to all disciplines from the system level (see Fig. 3). This way, the traditional approach of interdisciplinary trades is avoided. Compatibility between the provided system level information and the calculated disciplinary analysis results is handled by the lower-level optimization formulation.

In addition, the MDO bilevel decomposition provides independent and concurrent local disciplinary optimization processes that can be taken advantage of for control design and to distribute the computational effort when the design process requires analysis at different flight conditions, as shown in Fig. 4.

B. FDC Design-Constraining Flight Conditions

In this paper, the critical flight condition analyses, both symmetric and asymmetric, are defined based on their interdisciplinary effect on the longitudinal and lateral-directional control surfaces sizing as presented in Table 1. They contain static, maneuver, inertia coupling, and dynamic considerations along the flight envelope and are valid for a large range of aircraft configuration and concepts [8,14–16]. Only primary design conditions are considered. Critical control failure cases are neglected because they represent secondary requirements and can be covered in great extent by open-loop and closed-loop dynamic requirements.

Longitudinal static considerations are aimed to maintain steady 1-g level flight, which can become highly demanding for the control

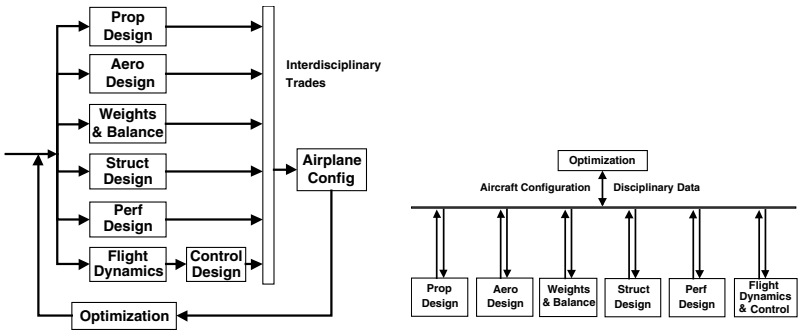

a) Traditional Design Process (Vertical Development)

b) MDO Design Process (Horizontal Development due to Variable Decoupling)

Fig. 3 Flight dynamics and control decoupling.

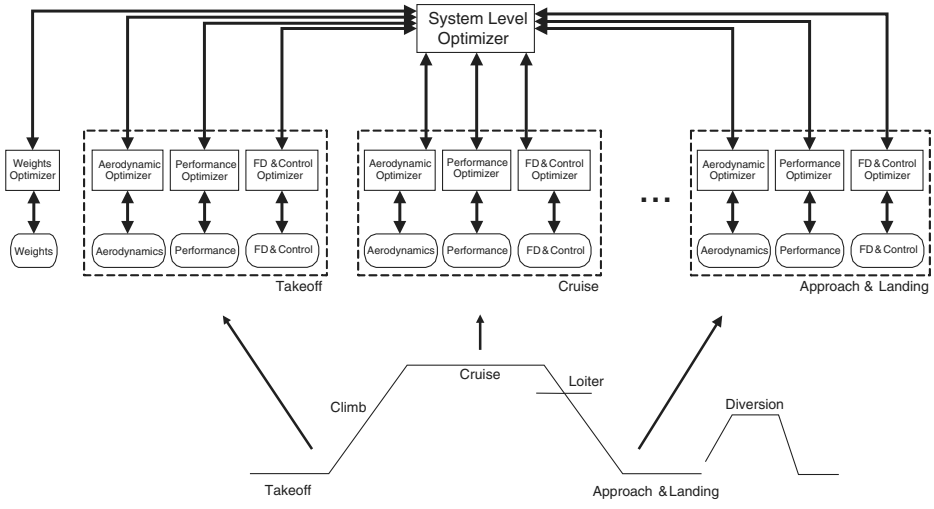

Fig. 4 Mission segments disciplinary decomposition.

Table 1 Longitudinal and lateral-directional design-constraining conditions

Control effector analysis	Applicable flight conditions	Critical CG location	Applicable requirement	Aircraft configuration
		Longitudinal		
1-g trim	All	Fwd, aft	FAR/JAR 25.161C	Dependent on flight condition
Approach 1-g trim	Approach	Fwd	FAR/JAR 25.161C	Full flaps
Landing 1-g trim	Landing	Fwd	FAR/JAR 25.161C	Full flaps, landing gear down
Go-around 1-g trim	Climb	Aft	FAR/JAR 25.161C	Full flaps, landing gear down
Maneuver load	All	Fwd	FAR/JAR 25.255	Dependent on flight condition
Go-around maneuver	Approach	Fwd	FAR/JAR 25.255	Full flaps
Rotation on takeoff	Takeoff	Fwd	FAR/JAR 25.143	Takeoff flaps, landing gear down, in ground effect
Rotation on landing	Landing	Aft	FAR/JAR 25.143	Full flaps, landing gear down, in ground effect
Dynamic mode oscillation	All	Fwd, Aft	FAR/JAR 25.181A	Dependent on flight condition
		Lateral		
Steady sideslip	All	——	FAR/JAR 25.177	Dependent of flight condition
One engine inoperative trim	All	——	FAR/JAR 25.161	Dependent of flight condition
Time to bank	All	——	FAR/JAR 25.147	Dependent of flight condition
Inertia coupling (pitch due to velocity axis roll)	Cruise	——	FAR/JAR 25.143	Dependent of flight condition
Yaw because of loaded roll pullout	Cruise	——	FAR/JAR 25.143	Dependent of flight condition
Coordinated velocity axis roll	Cruise	——	FAR/JAR 25.143	Dependent of flight condition
Dutch roll oscillation	All	——	FAR/JAR 25.181B	Dependent of flight condition
Roll subsidence	All	——	FAR/JAR 25.181B	Dependent of flight condition
Spiral divergence	All	——	FAR/JAR 25.181B	Dependent of flight condition
Closed-loop stability	All	——	FAR/JAR 25.177	Dependent of flight condition

effectors at low speeds in both forward (fwd) and aftward (aft) center of gravity (CG) limits, and with complex high-lift devices (where the aerodynamic pitching moment is large) as is the case in the approach and go-around flight phases. Maneuver considerations include load and rotation capabilities. In the first one the control effectors should be able to achieve load factors between the maximum and minimum operational limits in a pull-up from a dive over the flight envelope. This scenario becomes critical with the maximum takeoff weight and fwd CG, and in the go-around maneuver where the control effectors should be able to provide 8 deg/s^2 pitch acceleration starting from an approach trim condition. Rotation capabilities consider the ability of the control effectors to generate enough pitch moment to lift/derotate the nose wheel off/on the ground in takeoff and landing, respectively. This scenario becomes critical for takeoff at maximum gross weight with fwd CG, and with complex high-lift systems and high CG locations for landing. A pitch acceleration of 7 deg/s^2 for dry, prepared runways is specified for takeoff; it is higher than the minimum requirement as specified by Federal Aviation Regulations (FAR) 25.331C to provide an ample margin of control for future aircraft variants. Longitudinal dynamic response considerations are included as well for both the unaugmented (open-loop) and augmented (closed-loop) aircraft. With a control-augmented aircraft the closed-loop dynamic criteria assessment serves primarily for the evaluation of control laws. However, consideration of these conditions during the conceptual sizing stage ensures the aircraft is properly designed for adequate dynamic characteristics where control augmentation is used to avoid excessive system demands.

For the lateral-directional dynamics, the static considerations include steady sideslip and one-engine-inoperative (OEI) considerations. For the steady sideslip the lateral control surfaces should provide adequate roll and yaw power to perform steady sideslip maneuver at a 10-deg sideslip angle. This situation becomes critical during crosswind landing, when the sideslip angle is the greatest because of low airspeed. Similarly, the roll and yaw control effectors must be able to cope with asymmetric propulsion failure and maintain a steady straight flight with a 5 deg bank angle. This requirement becomes most demanding when operating at very low speed, specifically at takeoff where the weight and inertia are higher. A lateral-directional dynamic consideration is related to the time to bank response to full roll control input where the maneuver result must meet the performance requirements prescribed by [17]. Similar to the longitudinal case, critical dynamic characteristics are considered where the dynamic mode response for both the unaugmented (open-loop) and augmented (closed-loop) aircraft is assessed.

Three inertia coupling effects are included as well. The first one considers the pitch due to velocity axis roll, where the control effectors (elevators) should provide sufficient nose-down pitch authority to compensate for the nose-up moment as a result of inertia cross coupling during high angle-of-attack stability-axis roll maneuvers. Similarly, the control effectors (rudder) should possess adequate authority to overcome the yawing moment as a result of inertia coupling during a rolling pullout maneuver. In addition, the control effectors (rudder and ailerons) should be able to maintain a zero sideslip condition when performing a coordinated stability-axis roll.

Note that many of the above critical conditions for the control effectors match the traditional design mission profile flight phases which greatly simplify the flight condition analyses. However, if necessary other off-mission design conditions can be calculated and taken into consideration in the design process.

C. FDC Design Constraints and Requirements

Control power, which describes the efficiency of a control system in producing a range of steady equilibrium or maneuvering states [18] is defined as the common figure of merit to be used in FDC. It is quantified in terms of control deflection making it a continuous measurement useful for optimization. Specific sets of flight condition analyses will become critical, as the aircraft geometry varies during sizing. To ensure adequate flight control characteristics, the aircraft has to provide sufficient, yet not excessive, control power to meet the requirements of the prescribed flight analyses. For such reason, the FDC disciplinary constraints in (2) are specified in terms of such FOM, along with complementary open- and closed-loop dynamic requirements. The additional open-loop constraints take care of dynamic response specifications, such as limits of oscillation, damping ratios, natural frequency requirements, and control force gradients, which are defined from military specifications (such as [17]), or certification guidelines [such as FAR or JAR (joint aviation regulations)]. The closed-loop constraints are mainly aimed to meet with control design requirements to achieve internal stability of the control system, reject external disturbances, and assure adequate handling quality (HQ) requirements for both the longitudinal and the

lateral-directional modes. The assessment of HQ is closely related to dynamic considerations of the augmented closed-loop aircraft. Different handling quality quantification procedures exist. For the longitudinal case, the method such as the one proposed in [19] is very useful for an optimization procedure. It directly quantifies dynamic mode responses with HQ.

For example, if the aircraft dynamics is considered to be uncoupled into longitudinal and lateral modes, the short period mode handling quality can be assessed by using a control anticipation parameter (CAP). This parameter quantifies the response necessary to make precise adjustments to the flight path in terms of instantaneous angular pitching acceleration per unit of steady-state normal acceleration [20]. Furthermore, a generic control anticipation parameter (GCAP) extends the CAP application to both unaugmented and control-augmented aircraft [21]. The GCAP parameter is defined as

$$\text{GCAP} = \frac{\dot{q}(0)}{n_z(t_{\text{pk}})}\left[1 + \exp\left(\frac{-\zeta_{\text{sp}}\pi}{\sqrt{1-\zeta_{\text{sp}}^2}}\right)\right] \qquad 0 < \zeta_{\text{sp}} < 1 \tag{3}$$

where $n_z(t_{\text{pk}})$ is the normal acceleration at the peak time in response to a control step input. Specified GCAP bounds correlate the qualitative HQ levels (HQL) to the aircraft step input dynamic response. In the case of the Phugoid mode, handling quality is related to the mode damping and time to double the amplitude to ensure long enough time to stabilize the aircraft following a disturbance. Lateral HQ include roll and bank oscillation responses, a sideslip excursion, and "phi-to-beta" (ϕ/β) ratio criteria specifications [17,19].

D. Control System Design

Although some research has been done to select the most appropriate control system at the design stage before any detailed analysis is performed (see, e.g., [22]), the proposed methods do not perform the actual control design, therefore limiting their capability in the scope of control-configured aircraft design. Among the different control systems, the stability augmentation systems (SAS) have the strongest relationship with the design of the airplane, because their use can directly affect the aircraft layout characteristics. For this reason the control design goal at the conceptual design stage is to provide adequate stability augmentation systems to meet the close-loop and handling quality specifications over the flight envelope for both longitudinal and lateral dynamics. The aircraft plant is defined as a strictly proper linear time invariant (LTI) system without disturbances and sensor noise. An output feedback controller, Fig. 5, is used to provide the necessary stability augmentation. The feedback control is formulated as

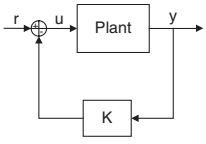

Fig. 5 Generalized control process.

$$\dot{\bar{x}} = A\bar{x} + B\bar{u}$$

$$\bar{y} = C\bar{x}$$

$$\bar{u} = \bar{r} - K\bar{y}$$

where

$$K = \begin{bmatrix} k_{11} & \cdots & k_{1d} \\ \vdots & \ddots & \vdots \\ k_{c1} & \cdots & k_{cd} \end{bmatrix} \tag{4}$$

where $\bar{x}$ is the aircraft states, $\bar{y}$ is the plant output, $\bar{u}$ is the control variables, c is the number of control variables $\bar{u}$, and d is the number of outputs $\bar{y}$. The closed-loop system is then

$$\bar{y} = C(sI - A_c)^{-1}Br \tag{5}$$

where

$$A_c = A - BKC$$

Stability is assured by selecting adequate control gains such that the closed-loop system lies in the negative real axis. It is assumed the aircraft dynamics follow "traditional" mode responses for both longitudinal and lateral dynamics so that the sign of the gains can be selected beforehand to guarantee stabilization. The control design itself is done as part of the MDO lower-level optimization, where control gains are specified as local optimization variables x in (2), whereas closed-loop stability and control constraints assure proper stabilization and performance.

IV. Application Example

A. Aircraft Mission and Optimization Goal

This section illustrates the proposed framework process in the case of a narrow-body 130-passenger airliner sizing, with twin wing engines, and conventional aft tail. Its mission profile is specified in Fig. 6, in line with industry standards for similarly sized aircraft. The design goal [MDO system level goal, Eq. (1)] is to find a feasible aircraft that maximizes specific air range ($\max_{z_{\text{SL}}, y_{\text{SL}}}$ range) while meeting individual disciplinary requirements as shown in the mission profile. A fixed fuel weight is specified as 40,000 lb, while the payload weight is specified as 32,175 lb based on 130 passengers, a crew of 2, and 5 attendants. The subsystem level disciplinary optimization process follows the formulation presented in Eq. (2).

B. Disciplinary Analyses

The design process of this example is composed of five coupled disciplines, namely, weights, aerodynamics, propulsion, performance, and dynamics and control. They are coupled as shown in the n-square diagram presented in Fig. 7. Details of each discipline are described below.

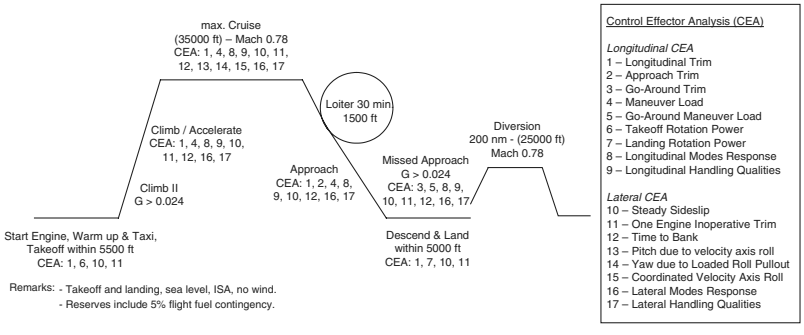

Fig. 6 Mission profile and longitudinal control effectors analysis considered.

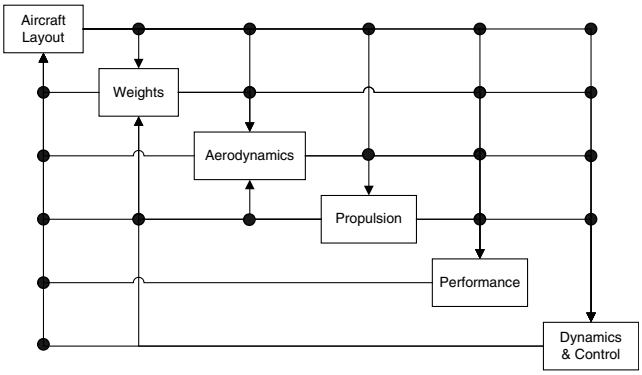

Fig. 7 Design example disciplinary couplings.

1) Weights: The aircraft takeoff weight is calculated from main component weights that are estimated using statistical methods [6,23]. The maximum permissible CG range for the configuration is calculated from each aircraft component permissible CG limits, based on their own geometry, physical, and functional considerations [24]. Similarly, the aircraft inertias are calculated from a buildup based on each component inertias calculated from the mean CG location for each component.

2) Aerodynamics: Aircraft lift, drag, and stability derivatives are calculated based on standard aerodynamic calculation used at the conceptual stage. Induced, parasite, and wave drag calculations are considered. The induced drag is calculated from parametric technology models whereas parasite drag is calculated using a detailed component buildup [25] taking into consideration viscous separation and components mutual interference effects. Transonic wave drag is modeled based on Lock's empirical approximation, using the Korn equation extended by Mason to include sweep [26]. To provide greater flexibility and accuracy in the calculation of aerodynamic characteristics, downwash effects, and stability derivatives, a combination of semi-empirical formulas [27,28] and a nonplanar multiple lifting surface panel method are implemented.

3) Performance: Takeoff and landing distances, rate of climb, and range are calculated based either on analytical expressions or numerical simulations. For example, takeoff distance is calculated based on a numerical simulation, while specific air range is calculated based on Breguet's equation. Landing field length is calculated assuming a landing weight of 90% maximum takeoff weight (MTOW).

4) Propulsion: Propulsion characteristics, such as engine weight, thrust, and specific fuel consumption for a given altitude and Mach number, are calculated based on engine scaling of a baseline PW-2037 high bypass turbofan engine.

5) Flight dynamics and control: For the present analysis it is assumed that all aircraft states are measurable without noise. Longitudinal and lateral design open-loop and closed-loop analyses are performed at each flight mission segment as shown on Fig. 6. Control design is performed for all in-flight phases (climb, cruise, and landing approach) of the mission profile.

C. Control Systems Design

In this example, the stability augmentation system uses standard cascaded SISO gains for the longitudinal and lateral-directional modes as shown in Fig. 8.

1. *Longitudinal Stability Augmentation*

Among the longitudinal modes the short period response is of prime concern due to its rapid response and its correlation with handling qualities evaluation. For this reason, efforts are concentrated in designing the SAS of this mode. The longitudinal short period flight dynamics equations can be formulated as [29]

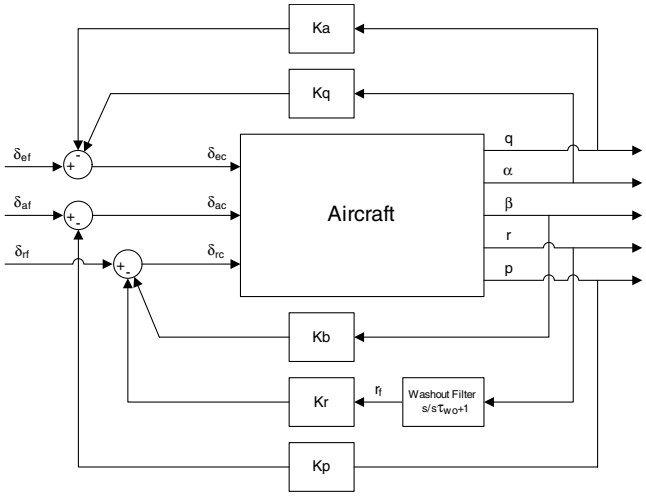

Fig. 8 Designed stability augmentation system.

$$\begin{bmatrix}\dot{\alpha}\\ \dot{q}\end{bmatrix}=\begin{bmatrix}Z_{\alpha/V} & 1\\ M_\alpha+M_{\dot{\alpha}}Z_{\alpha/V} & M_q+M_{\dot{\alpha}}\end{bmatrix}\begin{bmatrix}\alpha\\ q\end{bmatrix}+\begin{bmatrix}Z_{\alpha/V}\\ M_\delta+M_{\dot{\alpha}}Z_{\delta/V}\end{bmatrix}[\delta_e] \tag{6}$$

$[M_\alpha\ Z_\alpha\ M_{\dot{\alpha}}\ M_q]$ and $[M_{\delta_e}\ Z_{\delta_e}]$ are the dimensional stability derivatives and control derivatives respectively; their formulation includes the inertia terms, that is, $M_\alpha=(qS_{\text{ref}}\bar{c}/I_{yy})(\partial C_m/\partial\alpha)$.

Every dynamic state is affected by the elevator deflection control input signal. The control system is designed to achieve level 1 handling qualities performance while meeting natural damping and frequency limit characteristics. The output feedback gains can be expressed as

$$\{\bar{u}\}=\delta_e=\delta_{e_r}-\begin{bmatrix}k_\alpha & k_q\end{bmatrix}\begin{bmatrix}\alpha\\ q\end{bmatrix} \tag{7}$$

2. *Lateral-Directional Stability Augmentation*

The lateral flight control system provides lateral/directional stabilization. It consists of a roll feedback and yaw damper implemented to improve the Dutch roll damping. The washout filter time constant in the yaw damper depends on the washout corner frequency ω_{wo} as

$$\frac{1}{\tau_{\text{wo}}}=\omega_{\text{wo}}=k_{\text{wo}}\omega_{n_{dr}} \tag{8}$$

where k_{wo} is a control design variable representing a percentage of the Dutch roll natural frequency value.

The open-loop lateral dynamics equations are omitted but they follow the standard LTI state space form given as $\{\dot{\bar{x}}\}=[A]\{\bar{x}\}+[B]\{\bar{u}\}$, where $\{\bar{x}\}=[\beta\ p\ \phi\ r]^T$ and $\{\bar{u}\}=[\delta_a\ \delta_r]^T$. The lateral output feedback gains can be expressed as

$$\{\bar{u}\}=\begin{bmatrix}\delta_a & \delta_r\end{bmatrix}^T=\begin{bmatrix}\delta_a & \delta_r\end{bmatrix}_r^T-\begin{bmatrix}0\\ -k_r\omega_{\text{wo}}\end{bmatrix}x_5+\begin{bmatrix}0 & k_p & 0 & 0\\ k_\beta & 0 & 0 & k_r\omega_{\text{wo}}\end{bmatrix}\begin{bmatrix}\beta\\ p\\ \phi\\ r\end{bmatrix} \tag{9}$$

where x_5 is an additional state that arises from the inclusion of the washout filter in the state space representation. Note that as described

in Sec. III, the closed-loop system stability is guaranteed by selecting adequate control gain direction and values.

D. Design Variables and Constraints

Table 2 lists the design variables and their bounds used for the optimization. At the system level, 102 design variables are taken into consideration, from which 18 are global design variables and 84 are coupling design variables. The global design variables specify the general aircraft geometric configuration. Coupling variables include four flight condition independent terms (engine scaling factor (ESF), MTOW, fuel and engine weights), while the rest are distributed over the different flight conditions. Local variables are specified only to the flight dynamic and control discipline and correspond to the controller design gains (both longitudinal and lateral). Additional aircraft characteristics are provided as fixed parameters to the optimization problem. The nose landing gear location (xLG_{nose}) is assumed to be at 80% of the nose length: $xLG_{\text{nose}} = 0.8 * L_{\text{nose}}$. The main landing gear location (xLG_{main}) is calculated assuming that 8% of the maximum takeoff weight is applied on the forward wheels to provide sufficient weight on the nose wheel to permit acceptable traction for steering with the CG at its aft limit: $xLG_{\text{main}} = (x\text{CG}_{\text{aft}} - 0.08 * x_{n\text{LG}})/0.92$. The optimization constraints used at the subsystem level are shown in Table 3. They are split based on the analyzed disciplines and flight phase. The aerodynamic constraints are specified to avoid negative aerodynamic compressibility effects. The flight dynamic and control discipline include control power, and flight condition-dependent open and closed-loop dynamic constraints. The control power limits are set below the maximum control deflection, to provide allowance for additional control power requirements, such as active control and turbulence disturbance rejection, and a margin of safety for uncertainties on the stability and control derivative calculations. The normalized extension along the main control span (η_{ic} to η_{oc}), chord

Table 2 Variables names, units, bound, and initial points

Variable name	Variable type	Lower bound	Upper bound	Initial design
Wing reference area (S_w), ft^2	Global	1000	1400	1200
Wing aspect ratio (AR_w)	Global	7	11	9
Wing taper ratio (λ_w)	Global	0.1	0.4	0.2
Wing leading edge (LE) sweep angle (Λ_w), deg	Global	25	35	30
Wing average thickness/chord ratio (tc_w)	Global	0.08	0.12	0.1
Wing dihedral angle (Γ_w), deg	Global	−2	8	6
Wing location along fuselage ($xrLE_w$)	Global	0.3	0.5	0.4
Horizontal tail area (S_{ht}), ft^2	Global	200	350	300
Horizontal tail aspect ratio (AR_{ht})	Global	3	5	4
Horizontal tail taper ration (λ_{ht})	Global	0.3	0.6	0.4
Horizontal tail LE sweep angle (Λ_{ht}), deg	Global	25	40	35
Horizontal tail thickness/chord ratio (tc_{ht})	Global	0.07	0.11	0.09
Horizontal tail dihedral angle (Γ_{ht}), deg	Global	−2	3	0
Vertical tail area (S_{vt}), ft^2	Global	200	400	350
Vertical tail aspect ratio (AR_{vt})	Global	1.4	1.8	1.6
Vertical tail taper ratio (λ_{vt})	Global	0.3	0.6	0.4
Vertical tail LE sweep angle (Λ_{vt}), deg	Global	25	40	40
Vertical tail thickness/chord ratio (tc_{vt})	Global	0.09	0.12	0.11
Engine scaling factor (ESF)	Global	0.8	1.2	1
Maximum takeoff weight (MTOW), lb	Coupling	100,000	155,000	123,200
Engine weight (W_{eng}), lb	Coupling	5664	8670	7160
Thrust specific fuel consumption (TSFC), lb/hr/lb	Coupling	0.20	0.80	0.50
Engine thrust (T), lb	Coupling	20,000	35,000	31,000
Maximum clean lift coefficient ($CL_{\max}$)	Coupling	1.30	1.50	1.47
Lift to drag ratio (LD)	Coupling	6.00	15.00	9.00
Drag coefficient (CD)	Coupling	0.05	0.50	0.20
Stability derivative (Cz_α)	Coupling	4.00	6.50	5.50
Stability derivative (Cm_α)	Coupling	−2.00	2.00	−1.20
Stability derivative (CL_q)	Coupling	2.00	11.00	7.00
Stability derivative (Cm_q)	Coupling	−40.00	−10.00	−20.00
Stability derivative ($Cm_{\dot\alpha}$)	Coupling	−8.00	−0.10	−5.70
Stability derivative (Cz_{δ_e})	Coupling	0.05	0.50	0.33
Stability derivative (Cm_{δ_e})	Coupling	−2.00	−0.10	−1.00
Stability derivative (Cy_β)	Coupling	−1.50	−0.50	−1.17
Stability derivative (Cl_β)	Coupling	−0.30	−0.10	−0.26
Stability derivative (Cn_β)	Coupling	0.05	0.25	0.19
Stability derivative (Cl_p)	Coupling	−0.60	−0.30	−0.47
Stability derivative (Cn_p)	Coupling	−0.30	−0.10	−0.25
Stability derivative (Cl_r)	Coupling	0.25	0.85	0.57
Stability derivative (Cn_r)	Coupling	−0.40	−0.05	−0.19
Stability derivative (Cl_{δ_a})	Coupling	0.04	0.08	0.06
Stability derivative (Cn_{δ_a})	Coupling	−0.04	−0.01	−0.03
Stability derivative (Cy_{δ_r})	Coupling	0.10	0.30	0.26
Stability derivative (Cl_{δ_r})	Coupling	0.00	0.02	0.01
Stability derivative (Cn_{δ_r})	Coupling	−0.10	−0.01	−0.08
Control gain (k_α)	Local	−0.01	−50	0
Control gain (k_q)	Local	−0.01	−50	0
Control gain (k_p)	Local	0.01	0	50
Control gain (k_β)	Local	0.01	0	50
Control gain (k_r)	Local	−0.01	−50	0
Control variable (k_{wo})	Local	0.3	0.2	0.4

Table 3 Constraints for the optimization problem

Discipline	Flight phase	Constraint name	Value
Geometry	——	Wing span, ft	≤ 260
Geometry	——	Wing LE sweep, deg	$\leq$ H.T. (horizontal tail) LE sweep
Geometry	——	Wing LE edge sweep, deg	$\leq$ V.T. (vertical tail) LE edge sweep
Weights	——	Avail. wing fuel volume, ft^3	$\leq$ Req. block fuel volume
Weights	——	CG fwd position % mean aerodynamic chord (MAC)	≥ 0.05
Weights	——	CG aft position % MAC	≤ 0.55
Aerodynamics	Climb, cruise, approach, go-around	Wing Mach divergent drag no.	$\geq$ Mach no.
Aerodynamics	Climb, cruise, approach, go-around	H.T. Mach divergent drag no.	$\geq$ Mach no.
Aerodynamics	Climb, cruise, approach, go-around	V.T. Mach divergent drag no.	$\geq$ Mach no.
Performance	Takeoff	Takeoff field length, ft	≤ 5500 ft
Performance	Climb	Engine-out climb gradient	≥ 0.024
Performance	Go-around	Missed approach climb gradient	≥ 0.024
Performance	Landing	Landing field length, ft	≤ 5000 ft
Propulsion	All flight phases	Drag to thrust ratio	≤ 0.88
FDC	Climb, cruise, approach, go-around	Static margin	≥ 0.05
FDC	Takeoff	Rotation elevator power, deg	≤ 15
FDC	Landing	Rotation elevator power, deg	≤ 15
FDC	Climb, cruise, approach, go-around	1-g trim elevator power, deg	≤ 15
FDC	Climb, cruise, approach, go-around	Maneuver elevator power, deg	≤ 15
FDC	Climb, cruise, approach, go-around	Pitch-vel. axis roll elevator power, deg	≤ 15
FDC	Climb, cruise, approach, go-around	Steady sideslip aileron power, deg	≤ 20
FDC	Climb, cruise, approach, go-around	Steady sideslip rudder power, deg	≤ 15
FDC	Climb, cruise, approach, go-around	Steady sideslip roll angle, deg	≤ 5
FDC	Climb, cruise, approach, go-around	Engine-out trim aileron power, deg	≤ 20
FDC	Climb, cruise, approach, go-around	Engine-out trim rudder power, deg	≤ 15
FDC	Climb, cruise, approach, go-around	Yaw-loaded roll pullout, rudder power, deg	≤ 15
FDC	Climb, cruise, approach, go-around	Coord. vel. axis roll, aileron power, deg	≤ 20
FDC	Climb, cruise, approach, go-around	Coord. vel. axis roll, rudder power, deg	≤ 15
FDC	Climb, cruise	Open-loop short period damping ratio	$\geq 0.2, \leq 2.0$
FDC	Approach	Open-loop short period damping ratio	$\geq 0.35, \leq 2.0$
FDC	Climb, cruise, approach	Open-loop short period natural frequency	≥ 1
FDC	Climb, cruise	Open-loop short period GCAP for HQL 1	$\geq 0.038, \leq 10$
FDC	Approach, go-around	Open-loop short period GCAP for HQL 1	$\geq 0.096, \leq 10$
FDC	Climb, cruise, approach, go-around	Open-loop Dutch roll damping	≥ 0.02
FDC	Climb, cruise, approach, go-around	Open-loop Dutch roll natural frequency	≥ 0.5
FDC	Climb, cruise, approach, go-around	Open-loop time to roll, s	≤ 3
FDC	Climb, cruise, approach, go-around	Open-loop time to double spiral, s	≥ 8
FDC	Climb, cruise	Closed-loop short period damping ratio	$\geq 0.3, \leq 2.0$
FDC	Approach, go-around	Closed-loop short period damping ratio	$\geq 0.5, \leq 1.3$
FDC	Climb, cruise, approach, go-around	Closed-loop short period natural frequency	≥ 1
FDC	Climb, cruise	Closed-loop GCAP for HQL 1	$\geq 0.3, \leq 3.3$
FDC	Approach, go-around	Closed-loop GCAP for HQL 1	$\geq 0.16, \leq 3.6$
FDC	Climb, cruise, approach, go-around	Closed-loop Dutch roll damping	≥ 0.08
FDC	Climb, cruise, approach, go-around	Closed-loop Dutch roll natural frequency	≥ 0.5
FDC	Climb, cruise, approach, go-around	Closed-loop time to roll, s	≤ 1.4
FDC	Climb, cruise, approach, go-around	Closed-loop time to double spiral, s	≥ 12
FDC	Climb, cruise, approach, go-around	Closed-loop system eigenvalues	≤ 0

extension c_{ce}/c_{cs}, and maximum deflections of the control flapped surfaces are shown in Table 4. The deflection limits are specified to avoid nonlinear or undesirable aerodynamic behavior of the flapped surface.

E. Test Cases

Two illustrative cases are implemented to determine the relative merits of the proposed methodology. The first case optimizes the aircraft with the proposed FDC integration. The second case makes use of the same MDO architecture as the first one (disciplines are decoupled and decomposed) but it performs a traditional aircraft design sizing process where no considerations of FDC are made except for the use of tail volume coefficients to constrain the horizontal and vertical tail areas. Both cases are optimized from the same initial design point as shown in Table 2. To maintain uniformity in the calculations, a sequential quadratic programming (SQP) optimization algorithm [30] is used at both the system and the disciplinary levels. Proper scaling of the design variables, objectives, and constraints is enforced for the gradient-based optimizer to handle discrepancies along the feasible/near-feasible descent direction when disciplinary constraints force incompatibilities among the different subsystems. Objective function gradients are evaluated using finite differences. Tolerances for the optimization procedure are defined on the order of 10^{-6} based on initial studies to have a good compromise between the number of analysis calls at system and subsystem levels and the optimal objective function. Convergence of the optimization procedure is reached when the search direction, maximum constraint violation, and first-order optimality measure are less than the specified tolerances.

Table 4 Control effector flapped surface characteristics

Control effector/parameters	η_{ic}	η_{oc}	c_{ce}/c_{cs}	Max. deflection, deg
Elevator	0.25	0.95	30%	± 25
Ailerons	0.72	0.90	20%	± 25
Rudder	0.10	1.00	26%	± 15

V. Results

A. Optimized Designs and Comparisons

Table 5 shows selected variables and performance values for the multidisciplinary feasible solution obtained from both the integrated and traditional design test cases. The geometric configuration for both test cases is shown in Fig. 9. While similar wing characteristics

Table 5 Traditional and integrated FDC optimization results

Variable name	Traditional	Integrated FDC
Wing reference area (S_w), ft^2	1400	1400
Wing aspect ratio (AR_w)	11.00	11.00
Wing taper ratio (λ_w)	0.382	0.187
Wing LE sweep angle (Λ_w), deg	25.00	25.00
Wing average thickness/chord ratio (tc_w)	0.117	0.105
Wing dihedral angle (Γ_w), deg	2.000	4.839
Wing location along fuselage ($xrLE_w$)	0.39	0.35
Horizontal tail area (S_{ht}), ft^2	328.43	250.35
Horizontal tail aspect ratio (AR_{ht})	4.88	3.07
Horizontal tail taper ratio (λ_{ht})	0.561	0.525
Horizontal tail LE sweep angle (Λ_{ht}), deg	28.10	40.00
Horizontal tail thickness/chord ratio (tc_{ht})	0.088	0.073
Horizontal tail dihedral angle (Γ_{ht}), deg	0.00	−1.97
Vertical tail area (S_{vt}), ft^2	250.04	250.01
Vertical tail aspect ratio (AR_{vt})	1.8	1.4
Vertical tail taper ration (λ_{vt})	0.40	0.60
Vertical tail LE sweep angle (Λ_{vt}), deg	31.17	40.00
Vertical tail thickness/chord ratio (tc_{vt})	0.090	0.090
Engine scaling factor (ESF)	0.8	0.8
Maximum takeoff weight (MTOW), lb	120,186	120,413
Engine weight (W_{eng}), lb	5664	5664
Specific fuel consumption (TSFC) @ cruise, lb/h/lb	0.5034	0.5034
Engine thrust (T) @ takeoff, lb	25056	25056
Maximum clean lift coefficient (CL_{max}) @ cruise	1.483	1.501
Lift to drag ratio (LD) @ cruise	17.050	17.653
Drag coefficient (CD) @ cruise	0.020	0.019
Lift to drag ratio (LD) @ approach	9.681	10.311
Drag coefficient (CD) @ approach	0.183	0.143
Range, nm	5278.3	5788.7
Takeoff field length, ft	4284.1	4261.9
Landing field length, ft	3953.5	3945.2
Engine-out climb gradient	0.0681	0.0673
Missed approach climb gradient	0.0846	0.0906
Static margin @ cruise	0.3679	0.2424
Static margin @ approach	0.2528	0.1992

Table 6 Control power requirements comparison

Parameter	Traditional	Integrated FDC
Static margin @ cruise	0.3679	0.2424
Static margin @ approach	0.2528	0.1992
Takeoff rotation elevator power, deg	−6.2738	−14.0386
1-g trim elevator power, deg @ cruise	4.3247	4.3042
1-g trim elevator power, deg @ approach	19.6754	15.0588
Maneuver elevator power, deg @ cruise	−12.7531	−12.6707
Pitch-vel. axis roll elevator power, deg @ cruise	1.5796	2.7342
Pitch-vel. axis roll elevator power, deg @ approach	4.0268	6.4436
Steady sideslip aileron power, deg @ approach	**26.7672**	20.0638
Steady sideslip rudder power, deg @ approach	2.1798	6.5533
Steady sideslip roll angle, deg @ approach	4.1680	4.2251
Engine-out trim aileron power, deg @ approach	15.6064	18.5121
Engine-out trim rudder power, deg @ approach	**−28.1814**	−15.0702
Yaw-loaded roll pullout, rudder power, deg @ approach	−3.5798	−2.6306
Coordinated vel. axis roll, aileron power, deg @ approach	**23.3895**	16.5668
Coordinated vel. axis roll rudder power, deg @ approach	**−47.8037**	−13.0146

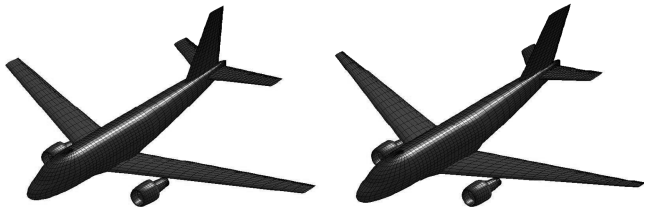

a) Traditional Design **b) Integrated FDC Design**

Fig. 9 Test cases optimal configurations.

are obtained for both designs, the horizontal and vertical tail geometry is significantly different as seen in Fig. 10. The concurrent consideration of flight dynamics and simultaneous design of stability and control augmentation systems leads to significant geometric changes over the traditional design approach. The horizontal tail area is reduced to promote lower static margins and improved aerodynamic efficiency. Similarly, the horizontal tail sweep increases to avoid flow separation at high Mach numbers, hence it aggravates changes in the wing pitching moment. In addition, the increase in horizontal tail sweep delays the stall angle and produces a more benign nonlinear lift/stall behavior. Furthermore, the wing apex location is moved slightly forward along with a horizontal tail area reduction. This affects the center of gravity of the aircraft and reduces its static margin. At the same time, the designed control system assures the required level of stability is achieved. The wing dihedral is increased significantly to improve roll stability characteristics. In terms of performance, both test cases meet the specified performance requirements. The reduction in exposed surface area for the integrated aircraft design causes higher lift to drag values at all flight conditions, as shown in Table 5. An air-range improvement of 510 nm is reached as compared to the traditional design approach.

Table 6 shows a control power requirement comparison between the two design cases, where bold values designate parameters which did not meet the required specifications (Table 3). The integrated design shows reduced static margins due to the horizontal area

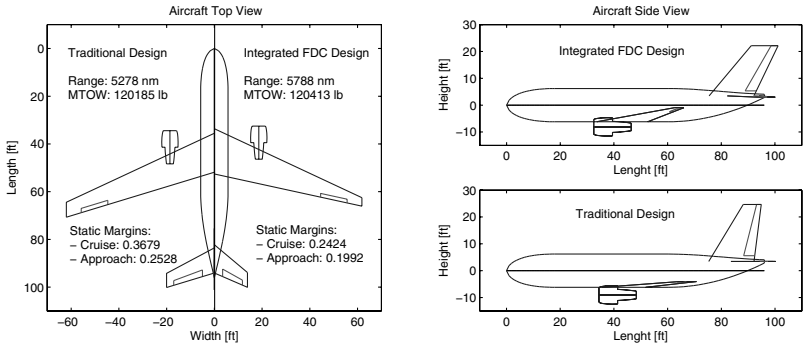

a) Top view **b) Side view**

Fig. 10 Aircraft configuration comparison.

Table 7 Open-loop dynamic properties comparison

Parameter	Traditional	Integrated FDC
Open-loop short period damping ratio @ cruise	0.3000	0.2874
Open-loop short period damping ratio @ approach	0.5272	0.4740
Open-loop short period natural frequency @ cruise	2.6409	2.1990
Open-loop short period natural frequency @ approach	1.5546	1.3677
Open-loop short period GCAP @ cruise	0.5152	0.3540
Open-loop short period GCAP @ approach	0.4042	0.3294
Open-loop Dutch roll damping @ cruise	0.1227	0.1247
Open-loop Dutch roll damping @ approach	0.1098	0.0777
Open-loop Dutch roll natural frequency @ cruise	0.8072	0.5024
Open-loop Dutch roll natural frequency @ approach	1.2906	1.2164
Open-loop time to roll, s @ cruise	0.2725	0.2878
Open-loop time to roll, s @ approach	0.4659	0.5842
Open-loop spiral time to double, s @ cruise	1030.9	32.239
Open-loop spiral time to double, s @ approach	19.5277	11.2838

Table 8 Integrated FDC closed-loop characteristics

Parameter	Cruise	Approach
k_α	−0.510	−1.000
k_q	−0.610	−1.000
k_p	1.201	1.301
k_β	1.021	0.001
k_r	−0.891	−0.591
k_{wo}	0.300	0.300
Closed-loop short period damping ratio	0.6066	0.5755
Closed-loop short period natural frequency	2.8929	1.8735
Closed-loop short period GCAP	0.6004	0.5926
Closed-loop Dutch roll damping	0.1604	0.1726
Closed-loop Dutch roll natural frequency	0.9438	0.9591
Closed-loop time to roll, s	0.1164	0.3256

reduction. The design requires larger elevator deflection for takeoff rotation as compared to the traditional aircraft, but it is still within limits of the specified deflection constraint. Trim requirements are similar for both designs. However, the integrated design requires less control power for trim at the approach condition, where the CG is critical at its maximum fwd position. Therefore, it provides a larger control power margin for other tasks such as gust disturbance rejection. For the lateral control power requirements, a significant difference can be seen between the two test cases. The traditional aircraft design approach cannot capture the flight dynamics coupling effects with the general airframe geometric characteristics or take advantage of control augmentation, leading to poor control power performance. For example, the aileron control power required for sideslip and the rudder control power required for engine-out trim exceeds the maximum allowable deflections at the approach condition. In this case, the aircraft is not able to maintain proper heading tracking when it lands with crosswinds or cope with an asymmetric propulsion failure. These characteristics are not considered directly in the traditional design process. The benefits of the integrated approach become evident because all control power requirements are met from the initial design phase. Furthermore, the required control deflections are lower than the allowable limits providing an ample margin of safety to deal with external disturbance rejection or to cope with an increased control effort due to failures. Additional open-loop dynamic results for both aircraft cases are shown in Table 7.

B. Integrated FDC Design Dynamic Behavior

Table 8 shows the optimal control gains and closed-loop characteristics of the integrated design. Aircraft flight dynamic characteristics are demonstrated using a simulation of the aircraft dynamics for cruise and landing approach representative conditions with and without the augmentation system. Longitudinal dynamic characteristics are shown in Figs. 11 and 12 for the cruise and approach flight phases, respectively. On both flight phases, the aircraft shows level 1 handling quality for both the bare-airframe and stability augmented system (Figs. 11a and 12a). Other flight conditions present a similar behavior. The response to an elevator step input by the augmented system is adequate, with fast damping of the disturbance as shown in Figs. 11b and 12b.

In a similar way, the response of the augmented aircraft to an aileron and rudder doublet control inputs are shown in Figs. 13 and 14 for the cruise and approach flight phases, respectively. It can be seen that the found lateral control augmentation system provides adequate control in both the roll and yaw rates, where the augmented system quickly damps out the commanded oscillations without significant overshoot.

C. Size Variation Effect on Integrated Methodology

The proposed integrated methodology was further applied over a broader set of aircraft sizes for the given configuration example. The aircraft size was varied to accommodate from 70 to 200 passengers. Variables and parameters such as payload and fuel weight were scaled in accordance with the variation of passengers. The effect of the methodology as compared to the traditional sizing process is shown in Fig. 15. The integrated approach leads to increase range as compared to the traditional process for all the aircraft size variations analyzed. As before, the integrated designs have reduced total control surface areas while the wing is shifted forward to take advantage of reduced static stability. By taking advantage of control-configuration interactions the design layout is altered to improve performance while meeting the specified disciplinary requirements.

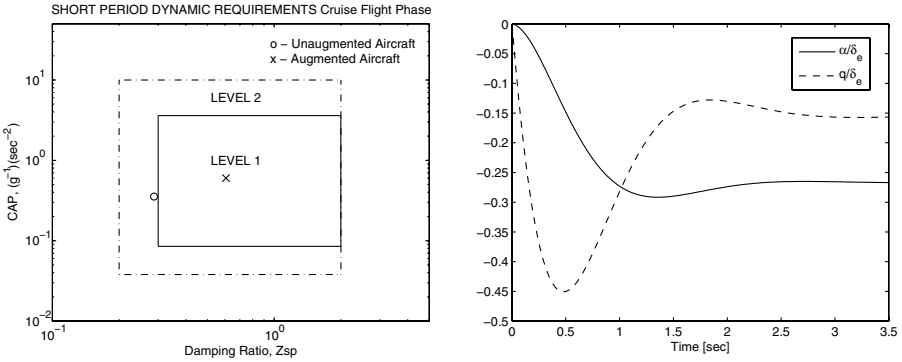

a) Short Period handling qualities **b) Closed-Loop response to control step**

Fig. 11 Cruise longitudinal dynamics characteristics.

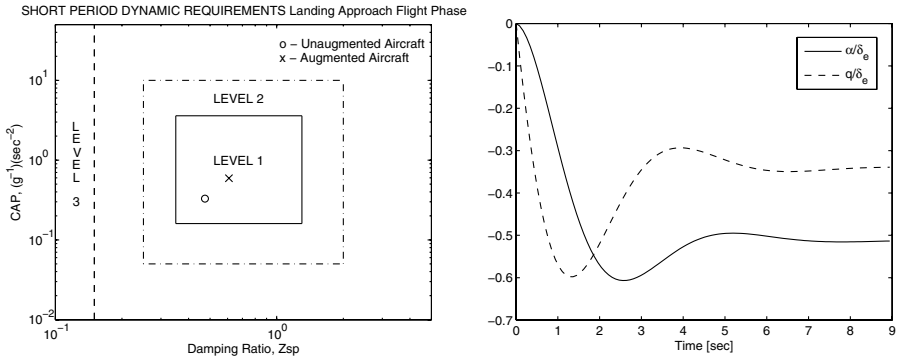

a) Short Period handling qualities **b) Closed-Loop response to control step**

Fig. 12 Landing approach longitudinal dynamics characteristics.

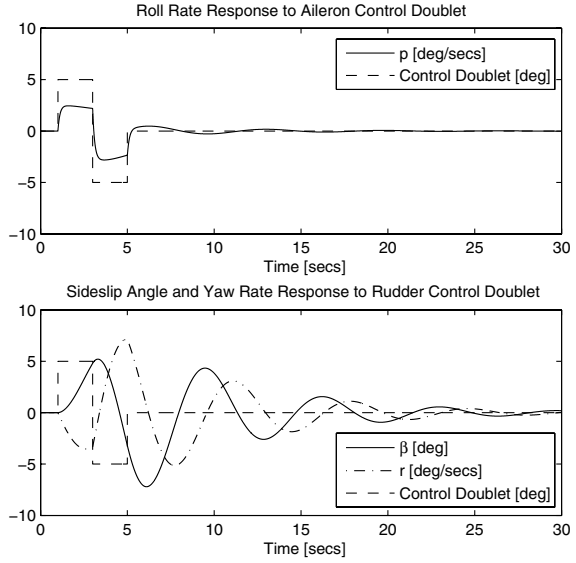

Fig. 13 Cruise closed-loop lateral dynamics response to controls doublet.

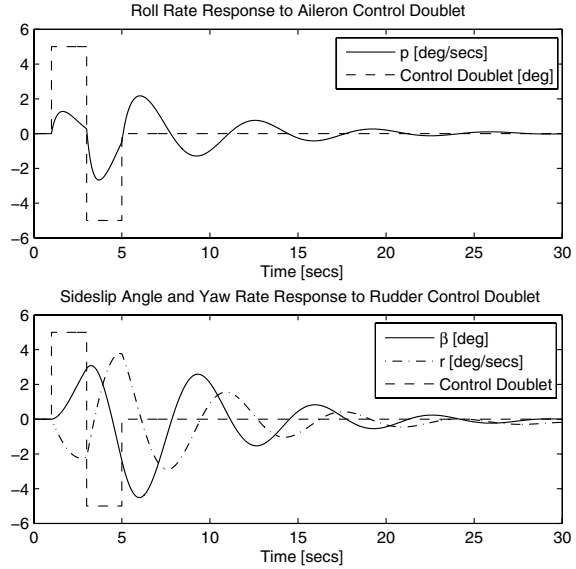

Fig. 14 Landing approach closed-loop lateral dynamics response to controls doublet.

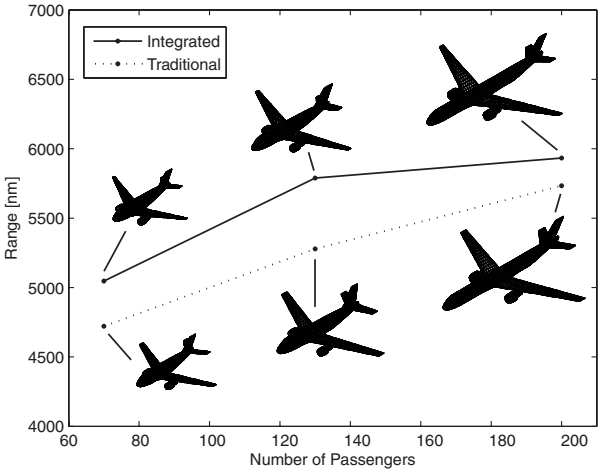

Fig. 15 Methodology effect on aircraft size variation.

VI. Conclusions

A methodology to address the challenges of integrating flight dynamics and control in the aircraft design sizing process has been presented. It enabled control-configuration considerations in the conceptual sizing process, while simultaneously designing proper control augmentation systems. The application of this approach to the design of a commercial aircraft was successful in producing solutions with better performance and flying characteristics than the traditional sizing process over a broad range of aircraft sizes. Furthermore, the methodology could potentially mitigate some of the problems that arise at the later stages of the design process as compliance with the most general flight dynamic certification requirements is assured from the conceptual stage, reducing time and cost in the engineering development cycle.

References

[1] Kehrer, W., "Design Evolution of the Boeing 2707-300 Supersonic Transport," *43rd AGARD Flight Mechanics Panel Meeting, Aircraft Design Integration and Optimization*, AGARD No. CP-147, Oct. 1973.

[2] Anon, *Current State of the Art On Multidisciplinary Design Optimization (MDO)*, General Publication Series, AIAA, Washington, D.C., Jan. 1991.

[3] Birkenstock, W., "Unstable Aircraft Design: The Computer at the Controls," *Flug Revue*, Vol. 9, Sept. 1999, p. 74.

[4] Dermis, T., Nalepka, J., Thompson, D., and Dawson, D., "Fly-by-Light: The Future of Flight Control Technology," *Technology Horizons Magazine, Air Force Research Laboratory Air Vehicles Directorate*, Report No. VA-04-12, April 2005.

[5] Nicolai, L., *Fundamentals of Aircraft Design*, 2nd ed., METS Inc., San

Jose, CA, 1984.
[6] Raymer, D., *Aircraft Design: A Conceptual Approach*, 3rd ed., AIAA Education Series, AIAA, Washington, D.C., 1999.
[7] Jenkinson, L., Simpkin, P., and Rhodes, D., *Civil Jet Aircraft Design*, 1st ed., Arnold, London, U.K., 1999.
[8] Kay, J., Mason, W., Lutze, F., and Durham, W., "Control Authority Issues in Aircraft Conceptual Design: Critical Conditions, Estimation Methodology, Spreadsheet Assessment, Trim and Bibliography," Virginia Polytechnic Institute and State University, TR VPI-Aero-200, Department of Aerospace and Ocean Engineering, Blacksburg, VA, Nov. 1993.
[9] Chudoba, B., *Stability and Control of Conventional and Unconventional Aircraft Configurations—A Generic Approach*, 1st ed., Books on Demand GmbH, Norderstedt, Germany, Jan. 2002.
[10] Sahasrabudhe, V., Celi, R., and Tits, A., "Integrated Rotor-Flight Control System Optimization with Aeroelastic and Handling Qualities Constraints," *Journal of Guidance, Control, and Dynamics*, Vol. 20, No. 2, March–April 1997, pp. 217–224.
[11] Holloway, R., and Burris, P., "Aircraft Performance Benefits from Modern Control Systems Technology," *Journal of Aircraft*, Vol. 7, No. 6, Nov.–Dec. 1970, pp. 550–553.
[12] Sobieszczanski-Sobieski, J., "Multidisciplinary Design Optimization: An Emerging New Engineering Discipline," NASA Langley Research Center, TM-107761, Hampton, VA, May 1993.
[13] Braun, R., Gage, P., Kroo, I., and Sobieszczanski-Sobieski, J., "Implementation and Performance Issues in Collaborative Optimization," AIAA, Paper No. 1996-4017, 1996.
[14] Chudoba, B., "Stability and Control Aircraft Design and Test Condition Matrix," Daimler-Benz Aerospace Airbus, TR EF-039/96, Hamburg, Germany, Sept. 1996.
[15] Chudoba, B., and Cook, M., "Identification of Design-Constraining Flight Conditions for Conceptual Sizing of Aircraft Control Effectors," AIAA Paper 2003-5386, 2003.
[16] Steer, A., "Design Criteria For Conceptual Sizing of Primary Flight Controls," *The Aeronautical Journal*, Vol. 108, No. 1090, Dec. 2004, pp. 629–641.
[17] "U.S. Military Handbook MIL-HDBK-1797," TR, Department of Defense, Washington, D.C., Dec. 1997.
[18] Etkin, B., and Reid, L., *Dynamics of Flight, Stability and Control*, 3rd ed., Wiley, New York, 1996.
[19] Anon, "MIL SPEC—Flying Qualities of Piloted Airplanes," U.S. Government Printing Office, TR MIL-F-8785C, Washington, D.C., Nov. 1980.
[20] Bihrle, W., Jr., "A Handling Qualities Theory for Precise Flight Path Control," Air Force Flight Dynamics Lab., TR AFFDL-TR-65-198, Wright–Patterson AFB, OH, June 1966.
[21] Gautrey, J., and Cook, M., "A Generic Control Anticipation Parameter for Aircraft Handling Qualities Evaluation," *The Aeronautical Journal*, Vol. 102, No. 1013, March 1998, pp. 151–159.
[22] Anderson, M., and Mason, W., "An MDO Approach to Control-Configured-Vehicle Design," AIAA Paper 1996-4058, 1996.
[23] Torenbeek, E., *Synthesis of Subsonic Airplane Design*, 6th ed., Delft Univ. Press and Kluwer Academic Publishers, Delft, The Netherlands, 1990.
[24] Chai, S., Crisafuli, P., and Mason, W., "Aircraft Center of Gravity Estimation in Conceptual Design," AIAA Paper 95-3882, 1995.
[25] Roskam, J., *Airplane Design*, 1st ed., Vol. 1–8, DARcorporation, Ottawa, KS, 1998.
[26] Malone, B., and Mason, W., "Multidisciplinary Optimization in Aircraft Design Using Analytic Technology Models," *Journal of Aircraft*, Vol. 32, No. 2, March–April 1995, pp. 431–438.
[27] Fink, R., "USAF Stability and Control DATCOM," TR Air Force Flight Dynamics Lab., Wright–Patterson AFB, OH, 1975.
[28] Engineering Sciences Data Unit, "Introduction to Aerodynamic Derivatives Equations of Motion and Stability," Engineering Sciences Data Unit International plc, TR 86021, London, U.K., 1987.
[29] Schmidt, L., *Introduction to Aircraft Flight Dynamics*, 1st ed., AIAA Education Series, AIAA, Reston, VA, 1998.
[30] Nocedal, J., and Wright, S., *Numerical Optimization*, 1st ed., Series in Operational Research, Springer–Verlag, New York, 1999.